Simultaneous quadrupole and octupole shape phase transitions in Thorium

Z. P. Li, B. Y. Song, and J. M. Yao

School of Physical Science and Technology,

Southwest University, Chongqing 400715, China

D. Vretenar

Physics Department, Faculty of Science,

University of Zagreb, 10000 Zagreb, Croatia and

Kavli Institute for Theoretical Physics China, CAS, Beijing 100190, China

J. Meng*

State Key Laboratory of Nuclear Physics and Technology,

School of Physics, Peking University, Beijing 100871, China

School of Physics and Nuclear Energy Engineering,

Beihang University, Beijing 100191, China and

Department of Physics, University of Stellenbosch, Stellenbosch, South Africa

Abstract

The evolution of quadrupole and octupole shapes in Th isotopes is studied in a fully microscopic framework based on nuclear Density Functional Theory. The constrained potential energy maps and observables calculated with microscopic collective Hamiltonians, indicate the occurrence of a simultaneous quantum shape phase transition between spherical and quadrupole-deformed prolate shapes, and between non-octupole and octupole-deformed shapes, as functions of the nucleon number. ^{224}Th is predicted closest to the critical point of the double phase transition. A microscopic mechanism of this phenomenon is discussed in terms of the evolution of single-nucleon orbitals with deformation.

PACS numbers: 21.60.Jz, 21.60.Ev, 21.10.Re, 21.10.Tg

*mengj@pku.edu.cn

Quantum phase transitions (QPTs) present a very active field of research in condensed matter, as well as in mesoscopic systems as, for instance, atomic nuclei, molecules, and atomic clusters. Nuclear QPTs, in particular, correspond to shape transitions between competing ground-state phases induced by variation of a non-thermal control parameter (number of nucleons) at zero temperature [1–5]. Most experimental and theoretical studies of first- and second-order nuclear QPT have considered quadrupole collective degrees of freedom, either for axially-symmetric deformed shapes [6–10] or triaxial shapes [11, 12]. Much less studied, although potentially very interesting, are transitions related to stable or dynamical octupole shapes (reflection-asymmetric, pear-like shapes). They have been analyzed employing phenomenological geometric models of nuclear shapes and potentials [13–17], algebraic models of nuclear structure [18] and, more recently, microscopic energy density functionals [19, 20]. In this Letter we report the first fully microscopic study of a simultaneous double QPT between spherical and quadrupole-deformed prolate shapes, and between non-octupole and octupole-deformed shapes in Th isotopes, located at ^{224}Th.

Studies of shape transitions usually start with the calculation of potential energy surfaces (PESs) as functions of collective deformation variables. The microscopic analysis of quadrupole and octupole shapes presented in this Letter is based on nuclear covariant density functional theory (CDFT) [21–23], which has successfully been applied to the description of a variety of structure phenomena all over the chart of nuclides.

In the present analysis the relativistic mean-field (RMF) implementation of the CDFT framework is employed using the functional PC-PK1 [24], and with pairing correlations treated in the BCS approximation. The microscopic PESs are obtained by performing constrained RMF+BCS calculations, with constraints on both quadrupole and octupole mass moments [25, 26]. To study the occurrence of possible phase transitions, one must analyze the behavior of observables that can be related to order parameters (equilibrium deformations, ground-state charge radii, excitation energies, electromagnetic transition rates, etc.). Observables that characterize low-lying collective excitations associated with quadrupole and octupole degrees of freedom are determined by the eigenstates of the corresponding generalized collective Hamiltonians (CH), with deformations as dynamical collective coordinates. The self-consistent solutions of constrained RMF+BCS calculations: single-particle wave functions, occupation probabilities, and quasiparticle energies that correspond to each point on the energy surface, are used to calculate, in the cranking approximation, the parameters

that determine the dynamics of the CH: the collective potential and inertia parameters as functions of collective coordinates. The diagonalization of the Hamiltonian yields the excitation energies and collective wave functions that are used to calculate observables [27, 28].

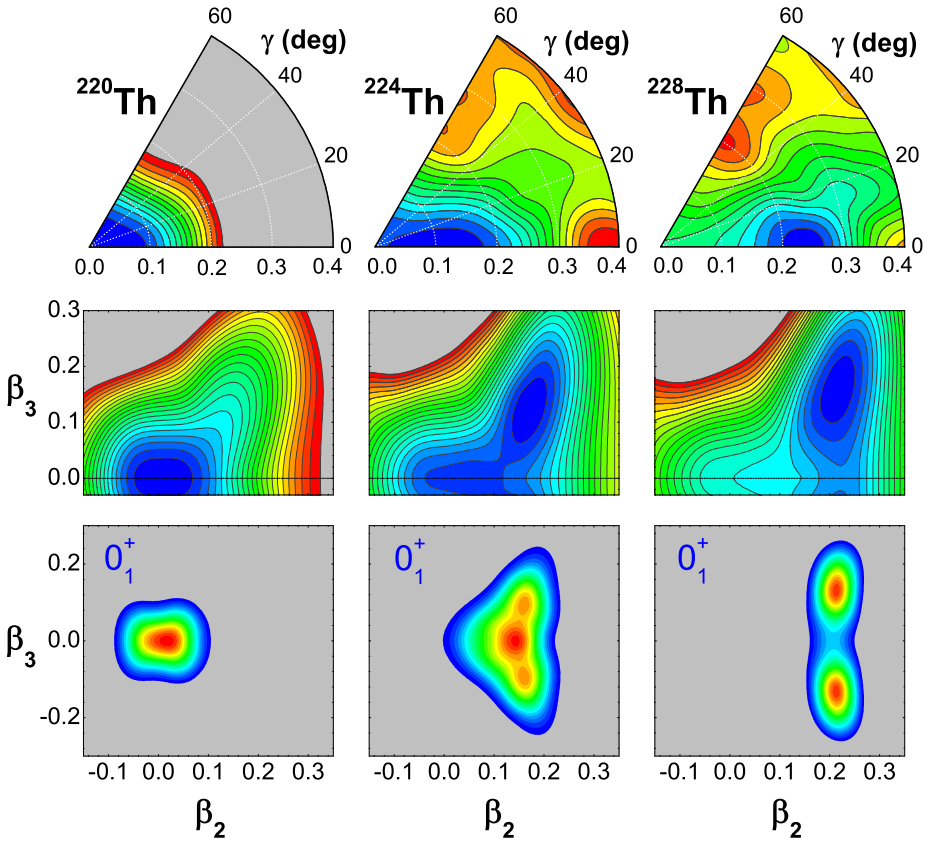

FIG. 1: (Color online) Self-consistent RMF+BCS triaxial quadrupole energy surfaces in the β_2-γ plane ($0 \leq \gamma \leq 60^0$) (upper panels), and axially-symmetric quadrupole-octupole energy surfaces in the β_2-β_3 plane (middle panels), for ^{220,224,228}Th. The contours join points on the surface with the same energy, and the separation between neighboring contours is 0.5 MeV. Probability density distributions in the β_2-β_3 plane for the ground states 0^+_1 of ^{220,224,228}Th (lower panels).

The self-consistent energy surfaces of ^{220,224,228}Th, calculated in the constrained RMF+BCS model with the PC-PK1 density functional in the particle-hole channel and a separable pairing force [29] in the particle-particle channel, are plotted in the panels of the upper two rows of Fig. 1. The contours join points on the surface with the same energy; successive contours differ in energy by 0.5 MeV. The upper panels display triaxial quadrupole

PESs in the β_2-γ plane. One notices the rather rapid transition from the spherical ^{220}Th to the well-deformed prolate shape of ^{228}Th. An interesting feature of the isotopic evolution is the flat prolate minimum in ^{224}Th, that extends in the interval $0 \leq \beta \leq 0.2$ of the axial deformation parameter. Flat-bottom potentials allow fluctuations in the deformation parameters and, therefore, indicate a possible phase transition. The quadrupole PES of ^{224}Th is reminiscent of those that we analyzed in the $N \approx 90$ region [30–32], in connection with first-order shape phase transitions between spherical and prolate axial shapes, first studied by Iachello using the square-well X(5) model [8].

If one considers ^{224}Th as a system at the X(5) critical point of a first-order shape phase transition then, noticing that the PES is rather steep in γ and in accordance with the X(5) model, the dependence of the PES on the two deformation parameters can be decoupled and, instead, the axially-symmetric PES in the β_2-β_3 plane analyzed. This is shown in the middle row of Fig. 1, where we plot the PESs of ^{220,224,228}Th calculated using the RMF+BCS model with constraints on the expectation values of the quadrupole moment $\langle Q_{20} \rangle$, and octupole moment $\langle Q_{30} \rangle$. The region of actinides with $N \approx 134$ is characterized by pronounced octupole correlations [33] and, indeed, our calculation shows a rapid shape transition between $N = 130$ to $N = 138$, from non-octupole to pronounced octupole deformations. The PES of the transitional nucleus ^{224}Th is rather soft with respect to the octupole deformation in the region $\beta_2 \sim 0.16$. This is consistent with the fact that in the Th isotopic chain the lowest excitation energy of the state 3^- is found in ^{224}Th [34]. The rapid transition and critical behavior can also be clearly seen in the probability density distributions in the β_2-β_3 for the ground states 0_1^+ of ^{220,224,228}Th, plotted in the lower panels of Fig. 1. The 0_1^+ states are eigenstates of the axially-symmetric quadrupole-octupole vibrational collective Hamiltonian (2DCH), with parameters determined by the self-consistent constrained RMF+BCS calculations. The probability densities of ^{220}Th and ^{228}Th isotopes peak at the spherical and stable quadrupole-octupole deformed shapes, respectively, whereas for ^{224}Th it is rather extended along both β_2 and β_3.

To disclose quantitative signatures of possible shape QPTs, we investigate the dependence of observables that can be related to order parameters as functions of the control parameter – nucleon number. A critical point of a QPT is characterized by a sudden change in the order parameter, even though one expects that in systems with a finite number of particles the transition is, to a certain extent, smoothed out. In Figure 2 we display the evolution with

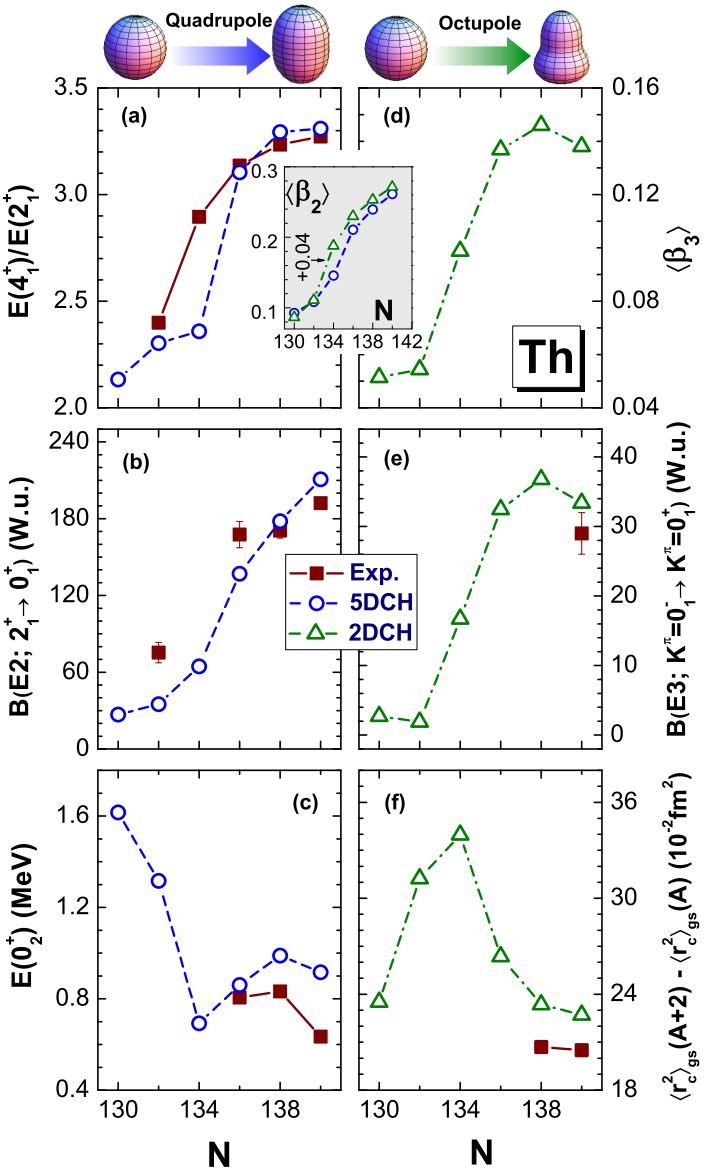

FIG. 2: (Color online) Evolution of the energy ratios $E(4_1^+)/E(2_1^+)$ (a), $B(E2; 2_1^+ \rightarrow 0_1^+)$ values (b), excitation energies of 0_2^+ states (c), expectation values of the octupole deformation parameter $\langle\beta_3\rangle$ in the ground state 0_1^+ (d), $B(E3; K^\pi = 0_1^- \rightarrow K^\pi = 0_1^+)$ (e), and the isotope shifts of the ground-state charge radii: $\langle r_c^2\rangle_{\rm gs}(A+2) - \langle r_c^2\rangle_{\rm gs}(A)$ (f), as functions of the neutron number in Th isotopes. Microscopic values calculated with the 5D and 2D collective Hamiltonians based on the PC-PK1 density functional are compared to available data. The inset shows the comparison between the expectation values of the quadrupole deformation parameter $\langle\beta_2\rangle$ calculated with the 5DCH and 2DCH.

neutron number of several quantities that are directly computed using the excitation ener-

gies and collective wave functions obtained with the 5DCH (for three-dimensional rotations and β_2-γ quadrupole vibrations) and the 2DCH (for axially-symmetric quadrupole-octupole vibrations). The parameters of the two Hamiltonians are completely determined by the self-consistent PESs calculated with the functional PC-PK1 (cf. Fig. 1). Figure 2 displays the isotopic dependence of the energy ratios $E(4_1^+)/E(2_1^+)$, $B(E2; 2_1^+ \rightarrow 0_1^+)$ values, excitation energies of 0_2^+ states, the expected octupole deformations $\langle\beta_3\rangle$ of the ground state 0_1^+, $B(E3; K^\pi = 0_1^- \rightarrow K^\pi = 0_1^+)$ values, and the isotope shifts of the ground state charge radii: $\langle r_c^2\rangle_{\rm gs}(A+2) - \langle r_c^2\rangle_{\rm gs}(A)$, for a sequence of Th nuclei. The calculated values are compared to available data. In general, the agreement between the theoretical results and the data is very good, especially considering that the calculation does not involve any additional parameter beside those used in the calculation of the self-consistent PESs.

An important result shown in Fig. 2 is that all the considered quantities present pronounced discontinuities at ^{224}Th. The panels on the left point to a phase transition between spherical and quadrupole-deformed prolate shapes, whereas the right panels reveal a phase transition from non-octupole to octupole-deformed shapes. For both shape QPTs ^{224}Th appears to be closest to the critical point. An exception is the energy ratio $E(4_1^+)/E(2_1^+)$ in ^{224}Th, which experimentally is close to the value of 2.9 predicted by the X(5) model [8] of the quadrupole QPT, whereas a much smaller value is calculated by the quadrupole 5DCH. However, as shown in the inset, this can simply be due to missing octupole correlations in the 5DCH calculation. The inset compares the expectation values of the quadrupole deformation parameter $\langle\beta_2\rangle$, calculated with the 5DCH and 2DCH. We notice that, in particular for ^{224}Th, the quadrupole-octupole Hamiltonian predicts a considerably larger value of $\langle\beta_2\rangle$, which would then translate in a larger value of the ratio $E(4_1^+)/E(2_1^+)$.

The quantities determined by the evolution of quadrupole-octupole correlations (panels on the right of Fig. 2), display a sudden change at ^{224}Th and then appear to saturate for heavier Th isotopes. We have, in fact, performed calculations up to $A = 234$ and found that the PESs in heavier nuclei become extended and soft with respect to β_3, but with almost constant $\beta_2 \sim 0.25 - 0.3$. Consequently, the excitation energy of the $K^\pi = 0_1^-$ vibrational state predicted by the 2DCH increases with mass number. This is consistent with the increase of the excitation energy of the experimental 1_1^- state (bandhead of $K^\pi = 0^-$ band), which has been interpreted as a signature of the transition from stable octupole deformations to octupole vibrations [13–16].

A microscopic picture of the softness of the potential with respect to both β_2 and β_3, and the related phenomenon of QPTs in ^{224}Th, emerges from the dependence of the single-nucleon levels on the two deformation parameters. In the upper and middle panels of Fig. 3 we plot the single neutron and proton levels of ^{224}Th along a path in the β_2-β_3 plane. The path follows the quadrupole deformation parameter β_2 up to the position of the equilibrium minimum $\beta_2 = 0.16$, with the octupole deformation parameter kept constant at zero value. Then, for the constant value $\beta_2 = 0.16$, the path continues from $\beta_3 = 0$ to $\beta_3 = 0.3$. In the lower panel of Fig. 3 we also show the evolution of the neutron and proton pairing energies, which reflect the level density around the Fermi surface (dash-dotted curves).

The extended quadrupole minimum in ^{224}Th (upper panel of Fig. 1) can be attributed to the wide region of low proton-level density around the Fermi surface, similar to the density of neutron levels in the rare-earth region at $N \approx 90$ for the X(5) QPT [30–32]. In the present case the Fermi surface for $Z \sim 90$ is far above the $Z = 82$ shell closure, but for small quadrupole deformations the splitting of the intruder state is not large enough to enhance the density of states. On the other hand, the single-neutron level density is determined by the $N = 126$ closure in lighter Th isotopes, and by the splitting of the intruder state $j_{15/2}$ in the heavier isotopes. Therefore, the lighter and heavier isotopes display nearly spherical and well-deformed prolate shapes, respectively. The emergence of soft octupole deformation (middle panel of Fig. 1) is determined by the evolution of levels along the β_3-path, that is, by the coupling between states of opposite parity that originate from the spherical levels $g_{9/2}$ and $j_{15/2}$ for neutrons, and $f_{7/2}$ and $i_{13/2}$ for protons [33].

In conclusion, using a fully microscopic theoretical framework based on nuclear CDFT, we have analyzed the evolution of quadrupole and octupole shapes in Th isotopes. The RMF+BCS calculations of constrained quadrupole triaxial and axially-symmetric quadrupole-octupole energy maps have been performed. The constrained RMF+BCS solutions determine the parameters of a quadrupole 5DCH, and a quadrupole-octupole 2DCH, that are used to calculate observables related to order parameters. Both the calculated PESs and the predicted observables (excitation energies, isotope shifts of charge radii, electromagnetic transition rates) indicate the occurrence of a simultaneous phase transition between spherical and quadrupole-deformed prolate shapes, and between non-octupole and octupole-deformed shapes, with ^{224}Th being closest to the critical point of the double QPT. A microscopic interpretation of the QPT has been given in terms of the evolution of single-

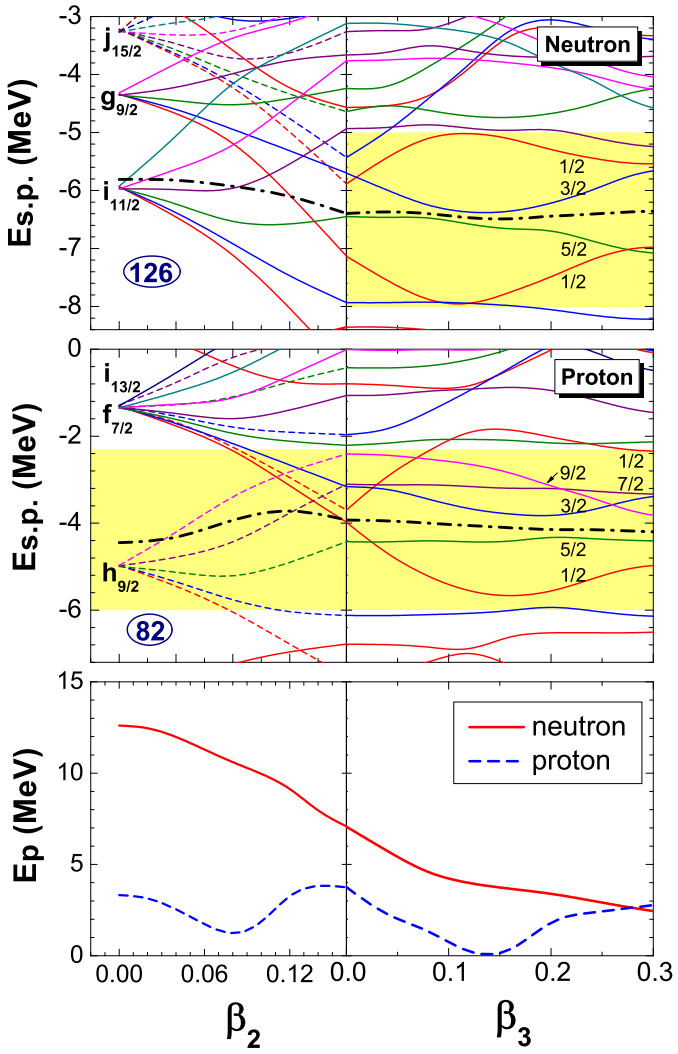

FIG. 3: (Color online) Single-neutron levels (upper panel), single-proton levels (middle panel), and neutron and proton pairing energies (lower panel) of ^{224}Th, as functions of the deformation parameters. Each plot follows the quadrupole deformation parameter β_2 up to the position of the equilibrium minimum $\beta_2 = 0.16$, with the constant octupole deformation parameter $\beta_3 = 0$ (left panels). For the constant value $\beta_2 = 0.16$, the panels on the right display the dependence of the single-nucleon energies and pairing energies on the octupole deformation, from $\beta_3 = 0$ to $\beta_3 = 0.3$. The thick dash-dotted (black) curves denote the Fermi levels.

nucleon orbitals with quadrupole and octupole deformation parameters. The results are in good agreement with experiment and with previous studies of shape transitions in this region. However, this is the first study in which both mean-field PESs and order parameters have been calculated fully microscopically, without any phenomenological control parame-

ter. Double shape QPT and related critical-point phenomena could occur in other finite quantum systems characterized by quadrupole and octupole collective degrees of freedom.

We thank B. N. Lu for helpful discussions. This work was supported in part by the Major State 973 Program 2013CB834400, the NSFC under Grant Nos. 10975008, 10947013, 11175002, 11105110, and 11105111, the Research Fund for the Doctoral Program of Higher Education under Grant No. 20110001110087, the Natural Science Foundation of Chongqing cstc2011jjA0376, and the Fundamental Research Funds for the Central Universities (XDJK2010B007 and DJK2011B002).

[1] F. Iachello, in Proceedings of the International School of Physics "Enrico Fermi" Course CLIII, A. Molinari, L. Riccati, W. M. Alberico and M. Morando (Eds.) IOS Press, Amsterdam 2003.

[2] R. F. Casten, Nature Physics 2, 811 (2006).

[3] R. F. Casten and E. A. McCutchan, J. Phys. G: Nucl. Part. Phys. 34, R285 (2007).

[4] P. Cejnar and J. Jolie, Prog. Part. Nucl. Phys. 62, 210 (2009).

[5] P. Cejnar, J. Jolie, and R. F. Casten, Rev. Mod. Phys. 82, 2155 (2010).

[6] F. Iachello, Phys. Rev. Lett. 85, 3580 (2000).

[7] R. F. Casten and N. V. Zamfir, Phys. Rev. Lett. 85, 3584 (2000).

[8] F. Iachello, Phys. Rev. Lett. 87, 052502 (2001).

[9] R. F. Casten and N. V. Zamfir, Phys. Rev. Lett. 87, 052503 (2001).

[10] J. Meng, W. Zhang, S. G. Zhou, H. Toki, and L. S. Geng, Eur. Phys. J. A 25, 23 (2005).

[11] J. Jolie, R. F. Casten, P. von Brentano, and V. Werner, Phys. Rev. Lett. 87, 162501 (2001).

[12] F. Iachello, Phys. Rev. Lett. 91, 132502 (2003).

[13] D. Bonatsos, D. Lenis, N. Minkov, D. Petrellis, and P. Yotov, Phys. Rev. C 71, 064309 (2005).

[14] D. Lenis and Dennis Bonatsos, Phys. Lett. B633, 474 (2006).

[15] P. G. Bizzeti and A. M. Bizzeti-Sona, Phys. Rev. C 70, 064319 (2004).

[16] P. G. Bizzeti and A. M. Bizzeti-Sona, Phys. Rev. C 77, 024320 (2008).

[17] R.V. Jolos, P. von Brentano and J. Jolie, Phys. Rev. C 86, 024319 (2012).

[18] S. Kuyucak and M. Honma, Phys. Rev. C 65, 064323 (2002).

[19] W. Zhang, Z. P. Li, S. Q. Zhang, and J. Meng, Phys. Rev. C 81, 034302 (2010).

[20] J. Y. Guo, P. Jiao, and X. Z. Fang, Phys. Rev. C 82, 047301 (2010).

[21] P. Ring, Prog. Part. Nucl. Phys. 37, 193 (1996).

[22] D. Vretenar, A. V. Afanasjev, G. A. Lalazissis, and P. Ring, Phys. Rep. 409, 101 (2005).

[23] J. Meng, H. Toki, S. G. Zhou, S. Q. Zhang, W. H. Long, and L. S. Geng, Prog. Part. Nucl. Phys. 57, 470 (2006).

[24] P. W. Zhao, Z. P. Li, J. M. Yao, and J. Meng, Phys. Rev. C 82, 054319 (2010).

[25] L. -S. Geng, J. Meng, and H. Toki, Chin. Phys. Lett. 24, 1865 (2007).

[26] B. -N. Lu, E. G. Zhao, and S. G. Zhou, Phys. Rev. C 85, 011301 (2012).

[27] T. Nikšić, Z. P. Li, D. Vretenar, L. Próchniak, J. Meng, and P. Ring, Phys. Rev. C 79, 034303 (2009).

[28] R. Rodríguez-Guzmán, L. M. Robledo, and P. Sarriguren, Phys. Rev. C 86, 034336 (2012).

[29] Y. Tian, Z. Y. Ma, and P. Ring, Phys. Lett. B676, 44 (2009).

[30] T. Nikšić, D. Vretenar, G. A. Lalazissis, and P. Ring, Phys. Rev. Lett. 99, 092502 (2007).

[31] Z. P. Li, T. Nikšić, Z. P. Li, D. Vretenar, J. Meng, G. A. Lalazissis, and P. Ring, Phys. Rev. C 79, 054301 (2009),

[32] Z. P. Li, T. Nikšić, Z. P. Li, D. Vretenar, and J. Meng, Phys. Rev. C 80, 061301(R) (2009).

[33] P. A. Butler and W. Nazarewicz, Rev. Mod. Phys. 68, 349 (1996).

[34] Brookhaven National Nuclear Data Center, http://www.nndc.bnl.gov (ENSDF).